International Journal of Minerals*, *Metallurgy and Materials
Volume 23*, *Number 3*, *March 2016*, *Page 247
DOI: 10.1007/s12613-016-1233-0

Innovative method for boron extraction from iron ore containing boron

Guang Wang, *Jing-song Wang*, *Xin-yun Yu*, *Ying-feng Shen*, *Hai-bin Zuo*, *and Qing-guo Xue*

State Key Laboratory of Advanced Metallurgy, University of Science and Technology Beijing, Beijing, 100083 China

(Received: 19 May 2015; revised: 19 July 2015; accepted: 27 July 2015)

Abstract: A novel process for boron enrichment and extraction from ludwigite based on iron nugget technology was proposed. The key steps of this novel process, which include boron and iron separation, crystallization of boron-rich slag, and elucidation of the boron extraction behavior of boron-rich slag by acid leaching, were performed at the laboratory. The results indicated that 95.7% of the total boron could be enriched into the slag phase, thereby forming a boron-rich slag during the iron and slag melting separation process. Suanite and kotoite were observed to be the boron-containing crystalline phases, and the boron extraction properties of the boron-rich slag depended on the amounts and grain sizes of these minerals. When the boron-rich slag was slowly cooled to 1100°C, the slag crystallized well and the efficiency of extraction of boron (EEB) of the slag was the highest observed in the present study. The boron extraction property of the slow-cooled boron-rich slag obtained in this study was much better than that of szaibelyite ore under the conditions of 80% of theoretical sulfuric acid amount, leaching time of 30 min, leaching temperature of 40°C, and liquid-to-solid ratio of 8 mL/g.

Keywords: ludwigite; reduction; melting separation; boron extraction

1. Introduction

Boron compounds, chiefly borates, are commercially important and have more than 300 commercial end uses. The worldwide consumption of borates is projected to increase in the subsequent years, and China is expected to substantially contribute to this increased consumption because of its large demand for borates [1]. China has a large amount of low-grade boron resources, which are difficult to economically exploit. The traditional high-grade boron resource of China, szaibelyite ore, will soon be exhausted at the present rate of consumption. Consequently, China is expected to import approximately (1.5–2) × 10^6 t of boron minerals in 2020. Ludwigite is a complex iron ore that is composed of iron, boron, magnesium, silica, etc. and is mainly found in China, USA, Italy, Sweden, Romania, and Russia. The Liaoning and Jilin Provinces of China contain 2.8 × 10^8 t of low-grade ludwigite deposits, which account for 57.88% of the boron reserves and 1% of the iron reserves in China. It is the main alternate boron resource of the future. However, ludwigite cannot be directly utilized as a single resource by traditional processing methods because of its low grades of total iron (TFe) and B_2O_3. The average composition of the ore is approximately 7wt% B_2O_3, 30wt% TFe, 24wt% MgO, and 15wt% SiO_2 [2−3]. In China, the comprehensive utilization of ludwigite is becoming increasingly urgent because of the increased demand for boron compounds and the depletion of the high-grade szaibelyite resource.

The key factors for the comprehensive utilization of ludwigite are a high degree of separation of the boron and iron elements and a high yield and good quality of the separated products. Many Chinese researchers have contributed to the development of methods and technologies to utilize ludwigite; these methods and technologies include magnetic separation [4], selective reduction and magnetic separation [5], hydrometallurgy [6], and blast-furnace reduction−melting separation [7−8]. The ore has a highly complex mineral phase composition, and the iron-containing minerals are finely embedded with the boron-containing minerals. Therefore, achieving a high degree of separation of boron and iron using the traditional ore dressing method is extremely difficult. The hydro-

---

Corresponding author: Hai-bin Zuo E-mail: zuohaibin@ustb.edu.cn

metallurgical method can perfectly separate boron and iron. However, the excessive acid consumption associated with this approach results in high costs, equipment erosion, and environmental pollution. The blast furnace method can also achieve a high degree of separation of boron and iron. However, the flowsheet for this process is very lengthy, running from agglomeration to blast furnace iron making, and the B_2O_3 content in the boron-rich slag is low because of the high coke ratio and because B_2O_3 is partially reduced into pig iron.

The rotary hearth furnace (RHF) coal-based direct reduction technology has been under development for approximately 40 years. It was initially used to treat iron-bearing metallurgical dust to recycle useful elements. However, RHF technology has rapidly been developed into a non-blast furnace ironmaking method that uses self-reducing composite pellets made of fine iron ore and pulverized coal as the feed [9−11]. If the furnace temperature is increased to 1350–1450°C, the reduced pellets will undergo iron and slag melting separation, namely, the iron-nugget process. It offers the benefits of a short flowsheet, a fast reaction rate, low raw-material requirements, and coke-free and flexible operation; furthermore, it is environmentally friendly [12−16].

In the present work, a novel flowsheet for the comprehensive utilization of ludwigite by carbon composite pellet reduction and melting separation technology (i.e., the iron-nugget process) is proposed. A schematic of the process flowsheet is shown in Fig. 1. As evident in the figure, initially, the reduction and melting separation of the ludwigite/coal composite pellet was performed to enrich boron into the slag. Next, the crystallization behavior and variation of the efficiency of extraction of boron (EEB) of the separated slag during slow cooling were studied. Finally, the acid-leaching behavior of the slow-cooled boron-rich slag was further investigated at the laboratory.

2. Experimental

2.1. Raw materials

The ludwigite iron concentrate used in this study was obtained from Dandong, Liaoning Province, China. The chemical composition of the complex ore sample is shown in Table 1. Mineralogical analysis of the concentrate was performed using X-ray diffraction (XRD; MAX-RB, 12 kW). The results presented in Fig. 2 indicate that the main crystalline phases were magnetite (Fe_3O_4), szaibelyite ($Mg_2(OH)(B_2O_4(OH))$), and chrysotile ($Mg_3(Si_2O_5)(OH)_4$). 98% of the iron ore concentrate particles were smaller than 0.074 mm.

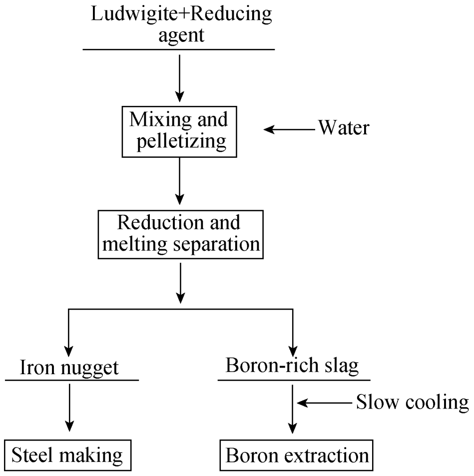

Fig. 1. Flowsheet of the novel boron extraction process of ludwigite.

Table 1. Chemical composition of ludwigite iron concentrate wt%

B_2O_3	TFe	MgO	SiO_2	Al_2O_3	FeO	CaO	P	S	LOI
6.90	47.20	19.20	5.32	0.15	18.90	0.34	0.020	0.16	4.97

Note: LOI stands for the mass loss on ignition.

The chemical composition of the reducing agent is listed in Table 2. The reducing agent was anthracite with high fixed carbon content and low sulfur content. All of the reducing agent particles passed 0.5 mm.

2.2. Experimental procedure

2.2.1. Reduction and melting separation experiments

The ludwigite iron concentrate and reducing agent were fully mixed. The mole ratio between the fixed carbon in the reducing agent and the oxygen of iron oxides in the iron concentrate was 1.2 to ensure complete reduction of iron oxide and carburization of the metallic iron. The moisture content of the mixture was controlled at 7wt%, and the mixture was again fully mixed. The resulting mixture was pelletized in a horizontal twin-roller machine under a pressure of 15 MPa. The size of the pillow-shaped pellet was 40 mm × 30 mm × 20 mm. The wet green pellet was dried at 120°C for 12 h before the reduction test. The reduction and melting separation experiments were performed in a closed $MoSi_2$ box resistance furnace to simulate the iron nugget production process of carbon composite pellets in rotary hearth furnace. A schematic of the experimental apparatus is shown in Fig. 3. In each run, the dry green pellet was placed into a graphite crucible and then heated in the furnace. The crucible was heated to the target temperature before the pellet was added to it. The graphite crucible protected the furnace from corrosion by the formed molten slag. The reduced sample was removed from the furnace at set time intervals and was cooled to ambient temperature under the protection of nitrogen to enable observation of the reduction and melting separation process.

2.2.2. Crystallization and EEB tests

The separated boron-rich slag from the reduction and melting separation experiment was smelted again in six graphite crucibles at 1400°C for 30 min in the $MoSi_2$ furnace. The mass of slag in each graphite crucible was approximately 20 g. After the six crucibles were heated, the furnace was powered off and allowed to slowly cool. One of the crucibles was removed from the furnace at each temperature of 1400, 1300, 1200, 1100, 1000, and 900°C and was subsequently quenched in water. The mineral composition of each quenched slag was characterized by XRD, and a scanning electron microscope (SEM, MLA 250) and an electron probe microanalyzer (EPMA, JXA-8230) were used to determine the microstructural evolution during the heating process.

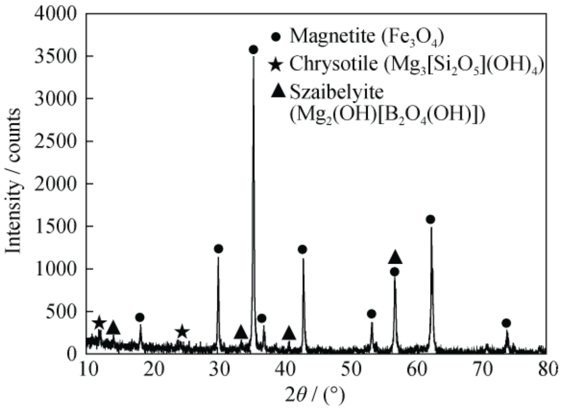

Fig. 2. XRD analysis of the ludwigite iron concentrate.

Table 2. Proximate and ash analysis of the reducing agent

Proximate analysis / wt%				Ash analysis / wt%					Ash fusibility / °C			
FC_d	V_d	A_d	S	SiO_2	Al_2O_3	Fe_2O_3	CaO	MgO	DT	ST	HT	FT
81.40	6.40	11.10	0.34	46.10	32.16	9.51	4.26	0.65	1300	1320	1350	1380

Note: FC_d represents the fixed carbon (dry basis), V_d the volatile matter (dry basis), A_d the ash (dry basis), S the total sulfur, DT the deformation temperature, ST the softening temperature, HT the hemispherical temperature, and FT the flowing temperature.

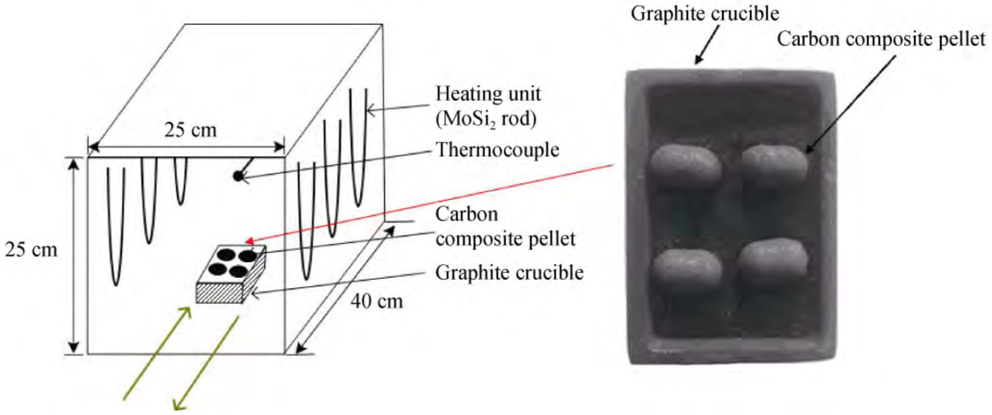

Fig. 3. Schematic of the experimental apparatus.

The normal-pressure alkaline leaching method was used to assess the EEB of the boron-rich slag. The parameters of the method are described as follows: quantity of boron-rich slag, 4.000 g; particle size of slag, 100% <0.074 mm; concentration of lye, 20wt% NaOH; volume of lye, 40 mL; leaching time, 4 h. The boron content of the primary and residual slag was analyzed using an inductively coupled plasma atomic emission spectrometer (ICP-AES). The EEB was defined as follows:

$$\text{EEB} = [(\text{Boron mass of primary slag} - \text{Boron mass of residual slag}) / \text{Boron mass of primary slag}] \times 100\% \quad (1)$$

2.2.3. Acid leaching experiments

Before the leaching experiments, the slow-cooled boron-rich slag (from 1400°C to room temperature) was ground to a particle size where 100% passed 0.074 mm. The chemical leaching experiment was conducted at a constant temperature that was maintained using a heating magnetic stirrer (DF-101S). Agitation was provided by a magneton, which enabled adequate dispersion of the slag particles in the acid solution. The stirring speed was set as 800 r/min. At the beginning of each trial, 10 g of boron-rich slag, along with distilled water, was added to an Erlenmeyer flask. The reaction time was recorded after sulfuric acid (98wt%) was added to the reaction mixture. At selected time intervals, a certain amount (500 μL) of the leaching solution was withdrawn by pipette and diluted to 50 mL in a volumetric flask. The boron concentration in the diluted solution was determined by ICP-AES, and the result was used to calculate the boron concentration in the leaching solution. The volume change due to the sample being withdrawn from the Erlenmeyer flask was not taken into account for the boron extraction determinations.

3. Results and discussion

3.1. Boron enrichment through reduction and melting separation

The separation of boron and iron from ludwigite is based on the premise of selective reduction. The standard molar Gibbs free energy for the reduction reactions of iron oxide and boron oxide by solid carbon are as follows [17]:

$Fe_3O_4 + C = 3FeO + CO$,

$$\Delta_r G_m^\ominus = 196720 - 199.38T, \text{ J/mol} \quad (2)$$

$FeO + C = Fe + CO$,

$$\Delta_r G_m^\ominus = 149600 - 150.36T, \text{ J/mol} \quad (3)$$

$B_2O_3 + C = B_2O_2 + CO$,

$$\Delta_r G_m^\ominus = 635931.14 - 324.8T, \text{ J/mol} \quad (4)$$

$B_2O_3 + 3C = 2B + 3CO$,

$$\Delta_r G_m^\ominus = 885375 - 470.14T, \text{ J/mol} \quad (5)$$

The reduction of B_2O_3 by solid carbon requires temperatures as high as 1600°C, and this reaction is substantially more difficult than the reduction of iron oxide. Traditionally, the reduction and melting separation temperature for the iron nugget process ranges from 1350 to 1450°C. Therefore, the selective reduction of iron oxide and boron oxide can be achieved in this process.

In the present work, the ludwigite/coal composite pellets were heated at 1400°C for various times. The volume of the pellet gradually shrinks during the reduction process and the surface of the pellet begins to melt after 9 min of heating. The slag and iron separate in a clean manner after 11 min of heating. The content of FeO in the slag decreases from 4.71wt% to 2.02wt% as the reduction time is increased from 11 min to 15 min [18].

SEM images of the microstructures of reduced pellets heated at 1400°C for 2, 4, 6, and 8 min are shown in Fig. 4. In the pellet reduced for 2 min, metallic iron exists primarily in the edge area around the boundary of coal particles and the size of the metallic iron particles is very small. No metallic iron remains in the center of the pellet and the center part remains near its original state because of the temperature difference across the pellet. In the case of the pellet reduced for 4 min, the amount of metallic iron in the edge area increases and a large quantity of unreduced iron oxide remains in the sphere. A small quantity of small particulate metal begins to appear in the center of the pellet. In the case of the pellet reduced for 6 min, the size of metallic iron increases and the compositional variation between the edge and center of the reduced pellet nearly disappears. In the case of the pellet reduced for 8 min, the metallic iron obviously aggregates and the slag phase appears, which indicates the onset of melting.

The iron nugget and the so-called boron-rich slag can be obtained when the pellet is reduced for 15 min at 1400°C. The chemical composition of the nugget is presented in Table 3. The yield of iron in the iron nugget form is 96.5%. Because of the short contact time between iron and slag and the thermodynamic difficulty of B_2O_3 reduction by carbon, the boron content in the nugget is only 0.065wt%. The chemical composition of the boron-rich slag is shown in Table 4. The content of B_2O_3 is greater than 20wt%, which is much higher than that obtained using the blast furnace process. The total yield of boron in the slag form is 95.7%, as determined using a mass balance calculation. Thus, most of the boron is concentrated in the boron-rich slag. We concluded that the degree of iron and slag separation in the iron nugget process is greater than that in the blast furnace process, where 10% of the total boron is reduced into pig iron. The main reasons for this greater degree of separation may be the shorter reduction time, lower reduction temperature, and lower reduction potential compared to the blast furnace conditions.

The XRD pattern of the slow cooled boron-rich slag is shown in Fig. 5. The crystalline phases in the slag are olivine (Mg_2SiO_4), suanite ($Mg_2B_2O_5$), and kotoite ($Mg_3B_2O_6$). The suanite is the main boron-containing crystalline phase. The EEB of the slow-cooled slag in this study is 86.46%. Thus, the slow-cooled slag crystallizes very well and can be used as a good raw material for boron extraction.

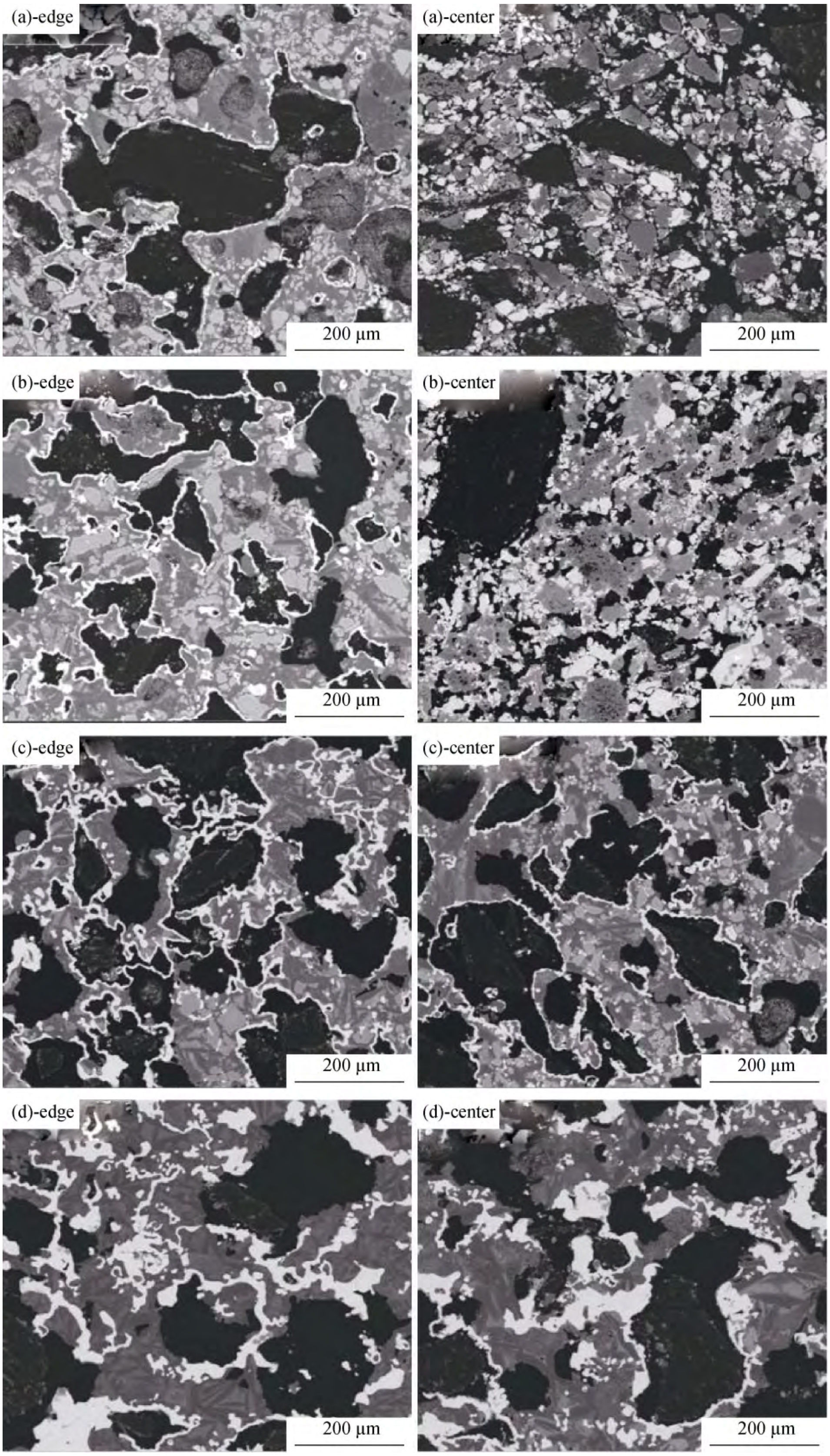

Fig. 4. Microstructures of the reduced pellets heated at 1400°C during the reduction process: (a) 2 min; (b) 4 min; (c) 6 min; (d) 8 min.

Table 3. Chemical composition of the iron nugget wt%

C	Si	Mn	B	S	P
3.57	0.018	0.038	0.065	0.27	0.079

Table 4. Chemical composition of the boron-rich slag wt%

MgO	B_2O_3	SiO_2	Al_2O_3	CaO	FeO	S
50.72	20.01	19.44	2.62	1.66	2.02	0.12

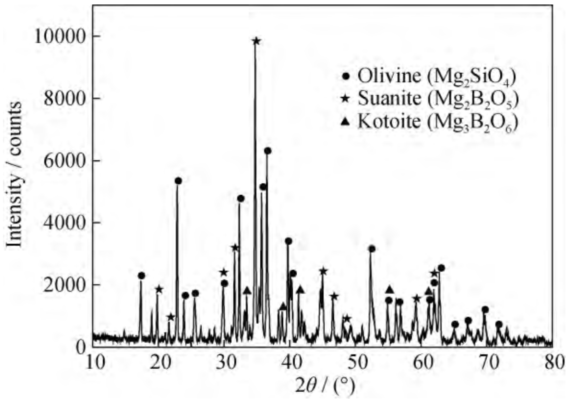

Fig. 5. XRD pattern of slow-cooled boron-rich slag.

The SEM and EPMA analysis results for the slow-cooled boron-rich slag sample are shown in Fig. 6 and Table 5. The micrograph reveals that the slag is composed primarily of four phases. Phases 1–3 are the main phases, representing nearly 95% of the total amount according to the image statistics of the area fraction of each phase. On the basis of the EPMA results, it can be concluded that phase 1 is suanite, phase 2 is kotoite, phase 3 is olivine, and phase 4 is an amorphous glass phase. The amount of the boron-bearing crystalline phase is similar to the amount of olivine. The glass phase contains a large amount of boron, and it is distributed in the gaps among the crystalline phases. Also, the boron-containing crystalline phase contains some SiO_2 and the olivine phase contains some B_2O_3. The morphology of the suanite particles is lath shaped, and most of the olivine and kotoite particles are square shaped. The embedded features of the three phases are comparatively simple. The grain sizes of suanite, kotoite, and olivine are as large as 100–200 μm.

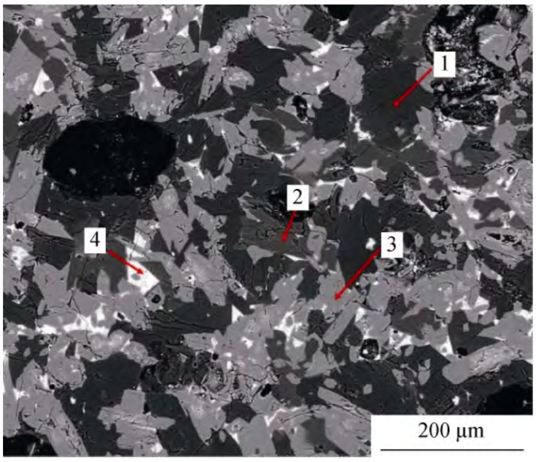

Fig. 6. SEM image of the slow-cooled boron-rich slag.

Table 5. EPMA analysis of the areas marked in Fig. 6

Area	Composition / wt%							Mineral phase	Content / %
	B_2O_3	MgO	SiO_2	CaO	Al_2O_3	FeO	MnO		
1	47.131	56.439	1.566	0.051	0.065	0	0.058	Suanite	34
2	37.322	60.726	0.605	0.038	0.060	0	0.041	Kotoite	11
3	3.140	48.262	35.051	0.064	0.419	0	0.028	Olivine	50
4	26.310	6.757	7.800	25.825	6.460	5.774	4.341	Glass	5

3.2. Crystallization behavior of the boron-rich slag

3.2.1. XRD analysis

The phase evolution of the slag during the slow-cooling process was investigated by XRD; the results are shown in Fig. 7. As evident in the figure, the phase compositions of the slag obviously change at different temperatures during slow cooling. For the slag quenched at 1400°C, the main crystalline phase is olivine. The main crystalline phase of the slag quenched at 1300°C is also olivine, and the intensity of its peak increases somewhat. The slag quenched at 1200°C also appears to contain an olivine crystalline phase, but the intensity of its peak decreases, and a new kotoite phase begins to appear. In the slag quenched at 1100°C, a new suanite phase begins to appear in large quantities and the olivine and kotoite phases appear as well. For the slags quenched at 1000 and 900°C, the phase species and the intensity of their peaks remain stable. The peak intensity of suanite is the greatest in the pattern of the slag sample cooled to room temperature. These analysis results indicate that the temperature range from 1300 to 1100°C is the most important range for the crystallization of the boron-containing phases during the cooling process.

3.2.2. SEM analysis

The microstructure of the quenched slag during slow cooling is shown in Fig. 8. The result shows that the microstructure of the slag also changes obviously at different temperatures during slow cooling. At 1400°C, the main phase in the slag is granular olivine. Some of the olivine exhibits a large crystal size with a square shape because it does not melt during melting separation. The remainder of the olivine exhibits a smaller particle size and precipitates during cooling. These substances, with the exception of the original olivine, may have been a liquid phase prior to water quenching. At 1300°C, the microstructure of the slag does not appreciably change and the amount of precipitated olivine increases. At 1200°C, a new phase with spatulate-shaped particles appears; according to the XRD results, this phase may be kotoite. The liquid phase still exists at this temperature. At 1100°C, the microstructure of the slag substantially changes and nearly all of the substances become crystalline. The suanite and kotoite both appear in large quantities and with large spatulate shape. At 1000°C, the size of the boron-containing crystalline particles decreases, especially their length, which is obviously shorter. The microstructure of the slag quenched from 900°C is similar to that of the sample slow-cooled to room temperature (Fig. 6).

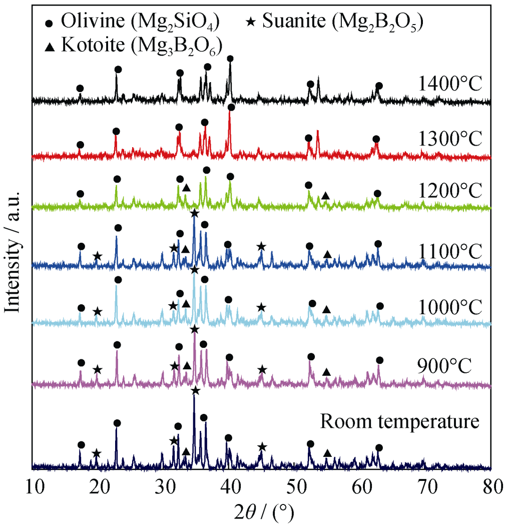

Fig. 7. XRD patterns of quenched slags during slow cooling.

The differential scanning calorimetry (DSC) curve of boron-rich slag during the heating process (20°C/min, SDT Q600) is shown in Fig. 9. As evident in the figure, the melting process of boron-rich slag consists of two steps. A small endothermic peak appears at 1211°C, which may result from the boron-rich phase with a low melting point. The second larger endothermic peak at 1243°C is the main melting peak. It can be concluded that the slag is in the molten state at temperatures above 1243°C except the original olivine during the slow-cooling process. Both the nucleation rate and the crystal growth rate are slow when the temperature is close to the melting point [18]. Thus, the amount of boron-containing crystalline phase is small when the temperature is greater than 1200°C.

3.2.3. EEB analysis

The variation of the EEB values of quenched slags during slow cooling is shown in Fig. 10. The EEB value of the slag quenched from 1400°C is only 46.4% because of its poor degree of crystallization; this EEB value is the lowest observed in the present study. The EEB value of the slag quenched from 1300°C increases slightly. The EEB value of the slag quenched from 1200°C increases to 76.9% because of the precipitation of kotoite. The EEB value of the slag quenched from 1100°C is 87.0% and is the highest value observed in the present study because of the extensive precipitation of suanite and kotoite. However, the EEB value of the 1000°C quenched slag decreases and the reason may be the decreasing size of the boron-containing crystalline phase. The EEB values of the quenched slags gradually increase during further cooling to temperatures below 1000°C. The reason for this variation of the EEB values is complicated, and Zhang and Sui [19] reported the same result that the highest EEB value of boron-rich slag occurs at 1100°C when a quenched amorphous $MgO–Al_2O_3–CaO–B_2O_3–SiO_2$ slag system is heated.

3.3. Acid leaching behavior of boron

3.3.1. Effect of the amount of sulfuric acid

The main reactions that occur between boron-rich slag and sulfuric acid during the leaching process are shown as follows:

$$2MgO\cdot B_2O_3 + 2H_2SO_4 + H_2O = 2H_3BO_3 + 2MgSO_4 \quad (6)$$

$$2MgO\cdot SiO_2 + 2H_2SO_4 = 2MgSO_4 + SiO_2 + 2H_2O \quad (7)$$

The theoretical amount of sulfuric acid in the acid leaching process, referred to as the amount consumed, is the amount required for the complete conversion of all metal cations in the ore into sulfates. In the present study, MgO represents nearly all of the basic metal oxide and the theoretical amount of sulfuric acid is defined as stoichiometric amount of H_2SO_4 for the complete reaction of MgO.

The boron extraction ratio of the slow-cooled boron-rich slag as a function of time when using 60% to 90% of the theoretical amount of sulfuric acid is presented in Fig. 11 under the conditions of leaching temperature of 30°C, leaching time of 55 min, and liquid-to-solid (L/S) ratio of 10 mL/g. The leaching rate of boron is large during the initial stage of the leaching process because of the higher initial sulfuric acid concentration. The boron extraction ratio increases with increasing sulfuric acid amount from 60% to 90% of the theoretical amount, and the boron extraction ratio after 55 min increases from 62% to 77%. The increase of the boron extraction ratio is not obvious when the sulfuric acid amount is increased from 80% to 90% of the theoretical amount. Therefore, the optimum amount of sulfuric acid in the leaching experiments of the boron-rich slag can be set as 80% of the theoretical amount, which is similar to the conclusion of a study on the preparation of boric acid from blast furnace boron-rich slag using the sulfuric acid method [20]. In the leaching process of practical boric acid production, the amount of sulfuric acid is approximately 60% to 80% of the theoretical amount. Excessive acid may result in greater corrosion of equipment and more impurities in the slag dissolving into solution [21].

3.3.2. Effect of leaching temperature

The effect of leaching temperature on the boron extraction ratio is shown in Fig. 12 under the conditions of 80% of the theoretical sulfuric acid amount, leaching time of 55 min, and L/S of 10 mL/g. The boron extraction ratio increases with increasing leaching temperature. The leaching temperature mainly affects the chemical reaction rate and diffusion

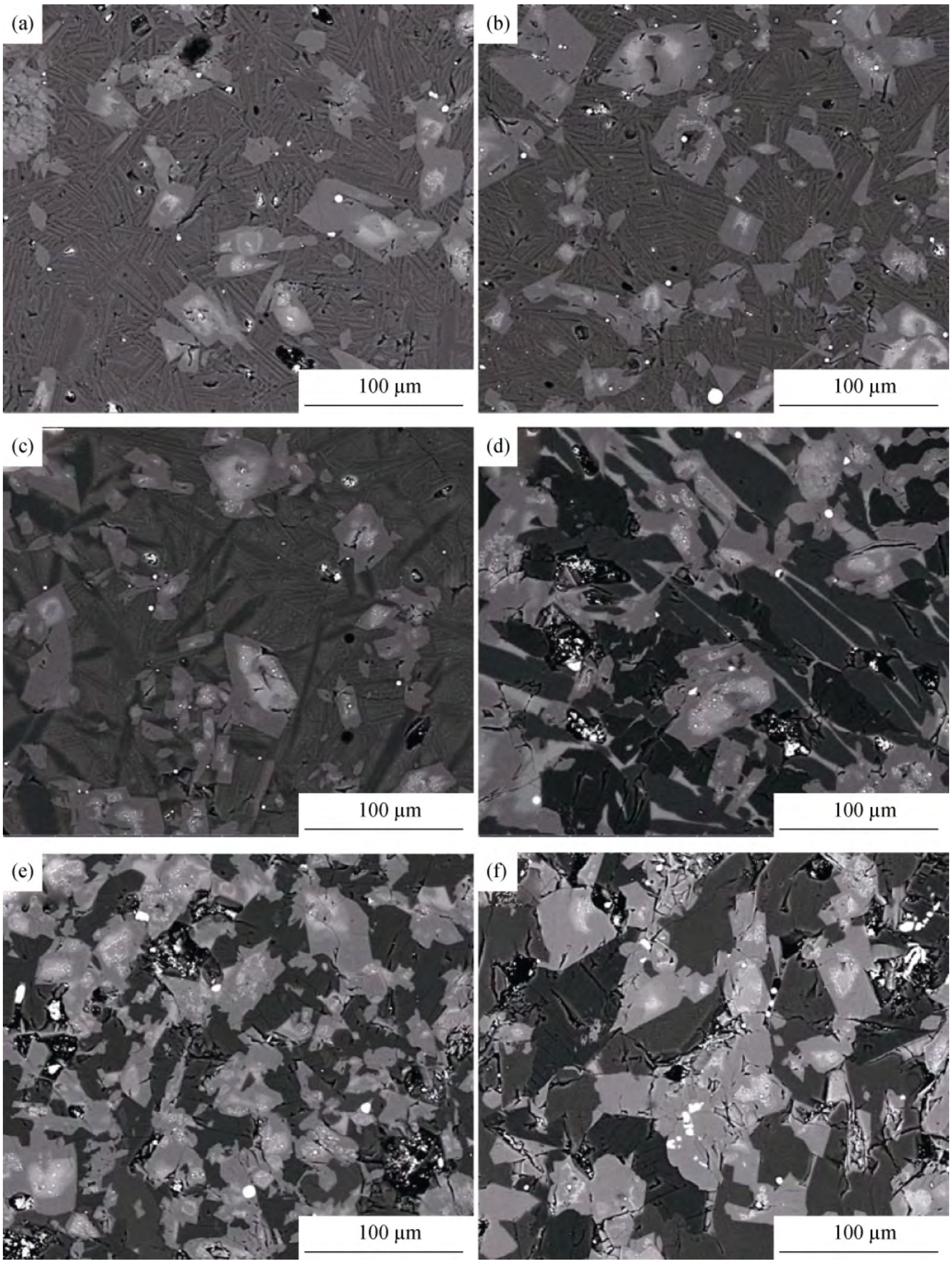

Fig. 8. Microstructure images of quenched slags during slow cooling: (a) 1400°C; (b) 1300°C; (c) 1200°C; (d) 1100°C; (e) 1000°C; (f) 900°C.

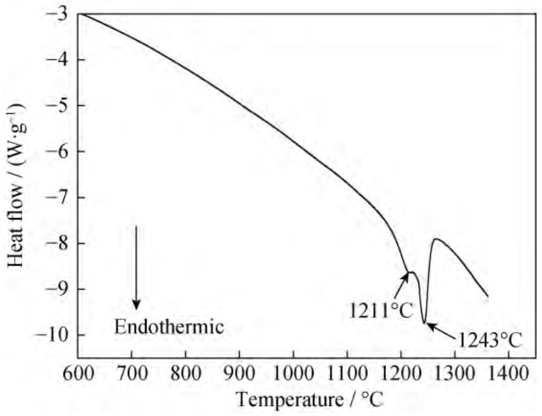

Fig. 9. DSC curve for the boron-rich slag.

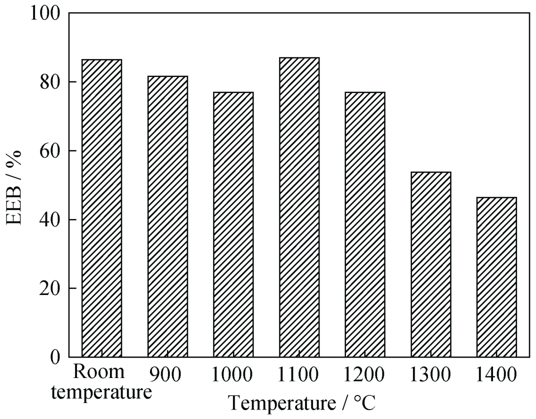

Fig. 10. Variation of EEB values of quenched slags during slow cooling.

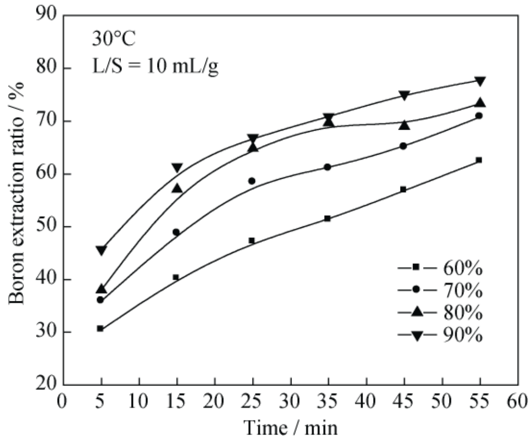

Fig. 11. Effect of sulfuric acid amount on boron extraction.

rate. Higher boron extraction ratio can be obtained at higher temperatures in the same leaching period. The leaching rate of boron stabilizes when the reaction is conducted for more than 35 min. When the leaching temperature is approximately 60°C, the rate of filtration is very slow. This slow filtration rate may be result of higher temperatures favoring the leaching of olivine, leading to formation of a silica sol during the leaching process. Therefore, the operating temperature for the sulfuric acid leaching of boron-rich slag should be kept below 60°C under the previously stated experimental conditions.

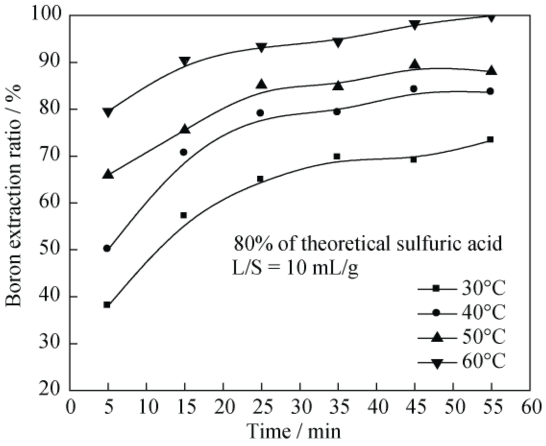

Fig. 12. Effect of leaching temperature on boron extraction.

3.3.3. Effect of L/S ratio

The effect of L/S ratio on the boron extraction ratio is shown in Fig. 13 under the conditions of 80% of the theoretical sulfuric acid amount, leaching time of 55 min, and leaching temperature of 40°C. The boron extraction ratio obviously increases when the L/S ratio is decreased from 10 to 8 mL/g and 97.2% of the boron in the slag has been extracted into the solution in less than 30 min. This extraction is a result of the reduced L/S ratio, which improves the acid concentration in the solution, benefiting the reaction between suanite and sulfuric acid. As the L/S ratio is further decreased to 6 mL/g, the boron extraction ratio does not significantly increases. The decrease of the L/S may also increase the leaching ratio of impurities, which adversely affects boron production. Moreover, when the L/S is 6 mL/g, the filtration rate appears to decrease because of the precipitation of boric acid from solution. Thus, the optimum L/S ratio of boron-rich slag leaching in sulfuric acid should be 8 mL/g according to the results of these leaching experiments. Actually, the L/S ratio in the boric acid production from szaibelyite using sulfuric acid leaching is 2 mL/g [21], which is much lower than the L/S ratio in the present study. In the experiments in this work, the boron extraction ratio can reach 98% under conditions of 80% of the theoretical amount of sulfuric acid, leaching time of 30 min, leaching temperature of 40°C, and an L/S ratio of 8 mL/g. It can be concluded that, for the production of boric acid, the boron extraction properties of the slow-cooled boron-rich slag obtained in this study are much better than szaibelyite ore in the sulfuric acid leaching process.

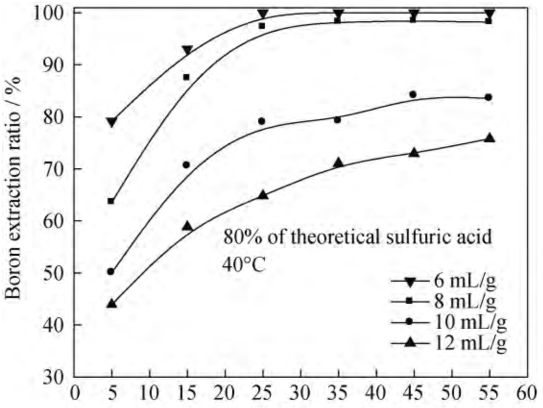

Fig. 13. Effect of the L/S ratio on boron extraction.

4. Conclusions

In this study, a novel boron enrichment and extraction process using ludwigite based on iron nugget technology has been investigated. The conclusions are summarized as follows:

(1) Ludwigite/coal composite pellets can realize iron and slag melting separation when reduced at 1400°C for 15 min, where 95.7% of the total boron in the ore will be enriched into the slag phase, forming boron-rich slag. The B_2O_3 content of the resulting slag is greater than 20wt%. The crystalline phases of boron-rich slag are olivine (Mg_2SiO_4), suanite ($Mg_2B_2O_5$), and kotoite ($Mg_3B_2O_6$). Suanite and kotoite are the boron-containing crystalline phase.

(2) The microstructure and phase composition of the boron-rich slag obviously change during the slow-cooling process from 1400 to 900°C. The original olivine exists in the initial molten slag because of its high melting point. Kotoite precipitates in small amounts at 1200°C, and suanite precipitates in large quantities at 1100°C. The slag quenched from 1100°C exhibits the best extraction properties.

(3) The optimal parameters for the boron extraction from boron-rich slag by sulfuric acid leaching are 80% theoretical sulfuric acid amount, leaching time of 30 min, leaching temperature of 40°C, and liquid-to-solid ratio of 8 mL/g. The boron extraction properties of the slow-cooled boron-rich slag are much better than those of the szaibelyite ore.

Acknowledgement

This work was financially supported by the National Natural Science Foundation of China (No. 51274033).

References

[1] S. Ken and K.M. Marcia, *Mineral Commodity Summaries*, U.S. Geological Survey, Reston, 2015, p. 32.

[2] X.P. Zhang, J.F. Lang, C.M. Cui, and S.L. Liu, Comprehensive utilization of low grade ludwigite ore with blast furnace smelting, *Iron Steel*, 30(1995), No. 12, p. 9.

[3] Z.T. Sui, P.X. Zhang, and C. Yamauchi, Precipitation selectivity of boron compounds from slags, *Acta Mater.*, 47(1999), No. 4, p. 1337.

[4] C.R. Wang and X.Q. Lian, On some problems of the beneficiation of boron iron ores, *Met. Mine*, 1995, No. 9, p.33.

[5] J.L. Zhang and H.T. Cai, Enrichment of boron in low-grade paigeite, *J. Univ. Sci. Technol. Beijing*, 31(2009), No.1, p. 36.

[6] R. Liu, X.X. Xue, T. Jiang, S.H. Zhang, and D.W. Huang, Comprehensive utilization of ludwigite and its prospect, *Multipurpose Util. Miner. Res.*, 2006, No. 2, p.33.

[7] S.L. Liu, C.M. Cui, and X.P. Zhang, Pyrometallurgical separation of boron from iron in ludwigite ore, *ISIJ Int.*, 38(1998), No. 10, p. 1077.

[8] Q.J. Zhao, Separating iron from boric iron ore by selective reduction, *J. Northeast. Univ. Technol.*, 11(1990), No.2, p.122.

[9] R. Zhu, J.T. Ren, G. Liu, T.J. Wan, and M. Xu, Development and practice on the rotary hearth furnace ironmaking process, *J. Univ. Sci. Technol. Beijing*, 29(2007), No. S1, p. 171.

[10] F.N. Griscom and D.R. Lyles, The Fastmet process-direct reduction technology for modern steelmaking, [in] *Proceedings of the 52nd Electric Furnace Conference*, Nashville, 1994, p. 75.

[11] K.Miyagawa, T. Matsumura, Y. Takenaka, and M. Shimizu, Development of the FASTMET as a new direct reduction process, [in] *Proceedings of the 2nd International Congress on the Science and Technology of Ironmaking*, Toronto, 1998, p. 877.

[12] S. Kikuchi, S. Ito, I. Kobayashi, O. Tsuge, and K. Tokuda, ITmk3 process, *Kobelco Technol. Rev.*, 2010, No. 29, p. 77.

[13] B. Anameric and S.K. Kawatra, Laboratory study related to the production and properties of pig iron nuggets, *Miner. Metall. Process.*, 23(2006), No. 1, p. 52.

[14] B. Anameric and S.K. Kawatra, The microstructure of the pig iron nuggets, *ISIJ Int.*, 47(2007), No. 1, p. 53.

[15] K. Nagata, R. Kojima, T. Murakami, M. Susa, and H. Fukuyama, Mechanisms of pig-iron making from magnetite ore pellets containing coal at low temperature, *ISIJ Int.*, 41(2001), No. 11, p. 1316.

[16] C.R. Borra, S. Dwarapudi, G. Kapure, V. Tathavadkar, and M.B. Denys, Effect of alumina on slag-metal separation during iron nugget formation from high alumina Indian iron ore fines, *Ironmaking Steelmaking*, 40(2013), No. 6, p. 443.

[17] Y.J. Liang and Y.C. Che, *Inorganic Thermodynamic Data Manual*, Northeastern University Press, Shenyang, 1993, p. 450.

[18] G. Wang, J.S. Wang, Y.G. Ding, S. Ma, and Q.G. Xue, New separation method of boron and iron from ludwigite based on carbon bearing pellet reduction and melting technology, *ISIJ Int.*, 52(2012), No. 1, p. 45.

[19] P.X. Zhang and Z.T. Sui, Effect of factors on the extraction of boron from slags, *Metall. Mater. Trans. B*, 26(1995), No. 2, p. 345.

[20] J. Li, L. Lei, L.J. Wang, T. Jiang, and Z.G. Fan, Study on preparation of boric acid from boric slag using sulfuric acid method, *J. Chin. Rare Earth Soc.*, 28(2010), Spec. Issue, p. 680.

[21] X.J. Zheng, *Production and Application of Borides*, Chemical Industry Press, Beijing, 2008, p. 114.